

# Investigation of pion-induced $f_1(1285)$ production off a nucleon target within an interpolating Reggeized approach

Xiao-Yun Wang<sup>1,\*</sup> and Jun He<sup>2,†</sup>

<sup>1</sup>*Department of Physics, Lanzhou University of Technology, Lanzhou 730050, China*

<sup>2</sup>*Department of Physics and Institute of Theoretical Physics, Nanjing Normal University, Nanjing, Jiangsu 210097, China*

In this work, the pion-induced  $f_1(1285)$  production off a nucleon target is investigated in an effective Lagrangian approach with an interpolating Reggeized treatment in a large range of the pion-beam momentum from threshold up to several tens of GeV. The  $s$ -channel,  $u$ -channel, and  $t$ -channel Born terms are included to calculate production cross sections. An interpolating Reggeized treatment is applied to the  $t$  channel, which is found to be important to reproduce the behavior of the existent experimental total cross sections at both low ( $\leq 8$  GeV) and high pion-beam momenta ( $\geq 8$  GeV). It is found that the  $t$ -channel contribution is dominant in the pion-induced  $f_1(1285)$  production at low beam momentum and still dominant at very forward angles at high momentum. The interpolated Reggeized treatment of the  $u$  channel is also discussed. The  $u$ -channel contribution is small and negligible at low momentum, and it becomes dominant at backward angles at momenta higher than 10 GeV. The differential cross sections are predicted with the model fixed by the fitting existent experimental data. The results are helpful to the possible experiments at J-PARC and COMPASS.

PACS numbers: 14.40.Be, 13.75.Gx, 12.40.Nn

## I. INTRODUCTION

The light meson is an important topic in hadron physics. The large nonperturbative effect in the light meson makes it relatively difficult to explore its internal structure. Due to the same reason, it is a wonderful place to study nonperturbative QCD. Though great progress has been achieved in the study of light meson spectroscopy during the last few decades, the internal structure of the light meson is still unclear, such as the debates about the  $\sigma(500)$ ,  $a_1/f_1(980)$ ,  $\kappa$ , and  $f_1(1285)$  [1]. Hence, many large experimental facilities will be working in this research area, such as LHCb, BelleII, and the CEBAF 12 GeV. In particular, a new detector GlueX has been installed at CEBAF after the 12 GeV upgrade, which will focus on the light meson study with electron or photon beams [2]. Like the light meson photoproduction off the nucleon, the pion-induced light meson production is also an important way to study the internal structure of the light meson. This process is accessible at J-PARC [3] and COMPASS [4] with high-energy secondary pion beams, which provide a good opportunity to study the light meson combined with the high-luminosity experiment at CEBAF with an electromagnetic probe.

Among the light mesons,  $f_1(1285)$  attracts much attention. Its internal structure has been studied for many years and is a long-standing problem. The Patrignani *et al.* (PDG) lists  $f_1(1285)$  as an axial-vector state with quantum number  $J^G(J^{PC}) = 0^+(1^{++})$  [5]. It has been suggested as a dynamically generated state produced from the  $K\bar{K}^*$  interaction in the literature [6–8]. In recent years, many XYZ particles were observed in the charmed and bottomed sector, such as  $X(3872)$ ,  $Z_c(3900)$ ,  $Z_c(4025)$ ,  $Z_c(10610)$ , and  $Z_c(10650)$  [9–12].  $f_1(1285)$  and these XYZ particles are close

to the  $K\bar{K}^*/D\bar{D}^*/B\bar{B}^*$  thresholds, respectively. The similarity in three flavor sections suggests that these particles are from the corresponding hadron-hadron interactions, which is supported by explicit calculations in the one-boson-exchange model [13–18]. In particular,  $f_1(1285)$  is the strange partner of the  $X(3872)$  as S-wave hadronic molecular states from the  $K\bar{K}^*$  and  $D\bar{D}^*$  interactions, respectively [13]. Compared with the XYZ particles in charmed and bottomed sectors,  $f_1(1285)$  is quite far from the  $K\bar{K}^*$  interaction. Hence, more investigation of  $f_1(1285)$  in different production processes may provide more helpful information to confirm the molecular state interpretation of  $f_1(1285)$ . Recently, the  $f_1(1285)$  meson was studied at CLAS in photoproduction from a proton target, and its decay pattern was extracted from high-precision data [19]. A nucleon resonance of a mass of about 2300 MeV was suggested in the analyses [19, 20]. However, a calculation with an interpolated Reggeized treatment suggests that the experimental cross section can be well reproduced without nucleon resonance included [21]. To check different models, an experimental study of pion-induced production process will be helpful.

Until now, there only exist some old experimental data and no explicit theoretical study of those data can be found in the literature to our knowledge [22–26]. Furthermore, it is promising to launch new measurements of the pion-induced  $f_1(1285)$  at J-PARC and COMPASS. Hence, it is interesting to analyze the pion-induced  $f_1(1285)$  production based on the old data in an effective Lagrangian approach to provide helpful predictions for the future experiment. Because the existing data scatter from near threshold to several tens of GeV, we will introduce the interpolating Reggeized treatment in the  $t$  channel as in the  $f_1(1285)$  photoproduction to reproduce the data at both low and high beam momentum [27]. The  $t$  channel and  $u$  channel usually correspond to the enhancement at forward and backward angles, respectively [28, 29]. The only existing data of the differential cross section are at very forward angles [23], which can be used to determine

\* xywang@lut.cn

† Corresponding author : junhe@impcas.ac.cn

the  $t$ -channel contribution. From the previous studies, the  $u$ -channel contributions will become more important at higher beam momentum [28, 29]. The  $u$  channel's contribution was found to be essential to interpret the behavior of the differential cross section of photoproduction [21]. Hence, in this work, we will consider the  $u$  channel as well as  $t$  and  $s$  channels to calculate the behavior of the pion-induced  $f_1(1285)$  production in a large range of the beam momentum. It can be expected that the Born  $s$  channel is negligible. Since the experimental data are very crude and information about the coupling constant is lacking, the  $s$ -channel nucleon resonance is not included in the current work as in the  $f_1(1285)$  photoproduction [21] to keep model simplified.

This paper is organized as follows. After the Introduction, we present the formalism including Lagrangians and amplitudes of pion-induced  $f_1(1285)$  production in Sec. II. The numerical results of cross sections are presented in Sec. III and compared with the existing data. Finally, the paper ends with a summary.

## II. FORMALISM

### A. Lagrangians

The basic tree-level Feynman diagrams for the  $\pi^- p \rightarrow f_1(1285)n$  reaction are depicted in Fig. 1. These include  $t$ -channel  $a_0(980)$  ( $\equiv a_0$ ) exchanges  $s$  and  $u$  channels with intermediate nucleon. As shown by PDG [5], the main two-body decay of  $f_1(1285)$  ( $\equiv f_1$ ) is the  $a_0\pi$  channel. Hence, only the  $a_0$  exchange is included in the  $t$  channel.

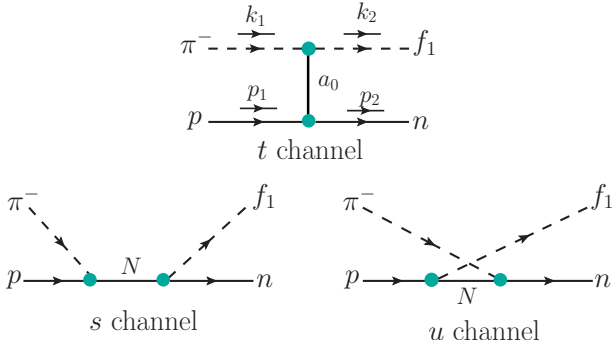


FIG. 1. Feynman diagrams for the  $\pi^- p \rightarrow f_1(1285)n$  reaction.

For the  $t$ -channel  $a_0$  exchange, one needs the following Lagrangians [30–32]

$$\mathcal{L}_{a_0NN} = g_{a_0NN} \bar{N} (\boldsymbol{\tau} \cdot \mathbf{a}_0) N, \quad (1)$$

$$\mathcal{L}_{f_1 a_0 \pi} = -g_{f_1 a_0 \pi} f_1^\mu \mathbf{a}_0 \cdot \partial_\mu \boldsymbol{\pi}, \quad (2)$$

where  $N$ ,  $f_1$ ,  $a_0$ , and  $\pi$  are the nucleon,  $f_1(1285)$ ,  $a_0(980)$  and  $\pi$  meson fields, respectively. The coupling constant  $g_{f_1 a_0 \pi}$  is determined from the decay width

$$\Gamma_{f_1 a_0 \pi} = g_{f_1 a_0 \pi}^2 \frac{(m_{f_1}^2 - m_{a_0}^2 + m_\pi^2)^2 - 4m_{f_1}^2 m_\pi^2}{24\pi m_{f_1}^4} |\mathbf{p}_\pi^{\text{c.m.}}|, \quad (3)$$

where  $\mathbf{p}_\pi^{\text{c.m.}}$  is the three-momentum of the pion in the rest frame of the  $f_1$  meson. By taking the value at PDG as  $\Gamma_{f_1 \rightarrow a_0 \pi} \simeq 8.71$  MeV [5], one gets a value of the coupling constant  $g_{f_1 a_0 \pi} \simeq 4.53$ . The coupling constant  $g_{a_0 NN}$  was not well determined in the literature [30, 31]. In the current work, we will take  $g_{a_0 NN}$  as a free parameter. For the  $t$ -channel  $a_0$  meson exchange, the general form factors  $F_{f_1 a_0 \pi} = (\Lambda_t^2 - m_{a_0}^2)/(\Lambda_t^2 - q_{a_0}^2)$  and  $F_{a_0 NN} = (\Lambda_t^2 - m_{a_0}^2)/(\Lambda_t^2 - q_{a_0}^2)$  are taken into account in this work and the cutoffs are taken as the same one for simplification. Here,  $q_{a_0}$  and  $m_{a_0}$  are the four-momentum and mass of the exchanged  $a_0$  meson, respectively.

To calculate the amplitude of the  $s$ -channel nucleon exchange, we need relevant Lagrangians. For the  $\pi NN$  interaction vertex we take the effective pseudoscalar coupling [33]

$$\mathcal{L}_{\pi NN} = -ig_{\pi NN} \bar{N} \boldsymbol{\gamma} \boldsymbol{\tau} \cdot \boldsymbol{\pi} N, \quad (4)$$

where  $\boldsymbol{\tau}$  is the Pauli matrix, and  $g_{\pi NN}^2/4\pi = 12.96$  is adopted [34, 35].

The Lagrangian of the  $f_1 NN$  coupling reads [36],

$$\mathcal{L}_{f_1 NN} = g_{f_1 NN} \bar{N} \left( f_1^\mu - i \frac{\kappa_{f_1}}{2m_N} \boldsymbol{\gamma}^\nu \partial_\nu f_1^\mu \right) \boldsymbol{\gamma}_\mu \boldsymbol{\gamma}^5 N + \text{H.c.}, \quad (5)$$

where  $g_{f_1 NN} = 2.5$  will be taken as discussed in Ref. [37]. Since the value of  $\kappa_{f_1}$  was determined by fitting the CLAS data in our previous work [21],  $\kappa_{f_1} = 1.94$  is adopted in this paper. For the  $s$  and  $u$  channels with intermediate nucleons, we adopt the general form factor to describe the size of the hadrons [38],

$$F_{s/u}(q_N) = \frac{\Lambda_{s/u}^4}{\Lambda_{s/u}^4 + (q_N^2 - m_N^2)^2}, \quad (6)$$

where  $q_N$  and  $m_N$  are the four-momentum and mass of the exchanged nucleon, respectively. Since the  $s$ -wave contribution is usually very small, we take  $\Lambda_s = \Lambda_u$ . The values of cutoffs  $\Lambda_s$ ,  $\Lambda_u$  and  $\Lambda_t$  will be determined by fitting experimental data.

### B. Amplitude for $\pi^- p \rightarrow f_1(1285)n$ reaction

The scattering amplitude of the  $\pi^- p \rightarrow f_1(1285)n$  process can be written in a general form of

$$-i\mathcal{M}_i = \epsilon_{f_1}^{\mu*}(k_2) \bar{u}(p_2) \mathcal{A}_{i,\mu} u(p_1), \quad (7)$$

where  $\epsilon_{f_1}^{\mu*}$  is the polarization vector of the  $f_1$  meson and  $\bar{u}$  or  $u$  is the Dirac spinor of the nucleon.

The reduced amplitudes  $\mathcal{A}_{i,\mu}$  for the  $s$ -,  $t$ -, and  $u$ -channel

contributions read

$$\mathcal{A}_{s,\mu}^{(N)} = -\sqrt{2}g_{\pi NN}g_{f_1 NN}F_s(q_N)\left(1 - i\frac{\kappa_{f_1}}{2m_N}\not{k}_2\right) \cdot \gamma_\mu \gamma^5 \frac{(\not{q}_N + m_N)}{s - m_N^2} \gamma_5, \quad (8)$$

$$\mathcal{A}_{t,\mu}^{(a_0)} = i\sqrt{2}g_{a_0 NN}g_{f_1 a_0 \pi}F_t(q_V)\frac{1}{t - m_{a_0}^2}k_{1\mu}, \quad (9)$$

$$\mathcal{A}_{u,\mu}^{(N)} = -\sqrt{2}g_{\pi NN}g_{f_1 NN}F_u(q_N)\gamma_5 \frac{(\not{q}_N + m_N)}{u - m_N^2} \cdot \left(1 - i\frac{\kappa_{f_1}}{2m_N}\not{k}_2\right) \gamma_\mu \gamma^5, \quad (10)$$

where  $s = (k_1 + p_1)^2$ ,  $t = (k_1 - k_2)^2$  and  $u = (p_2 - k_1)^2$  are the Mandelstam variables.

### C. Interpolating Reggeized $t$ channel

In this work, we will consider a large beam-momentum range from threshold to several tens of GeV. To describe the behavior of the hadron production at high momentum, the Reggeized treatment should be introduced to the  $t$  channel[39–43]. The Reggeized treatment for  $t$ -channel meson exchange consists of replacing the product of the form factor in Eq. (9) as

$$F_t(t) \rightarrow \mathcal{F}_t(t) = \left(\frac{s}{s_{scale}}\right)^{\alpha_{a_0}(t)} \frac{\pi\alpha'_{a_0}(t - m_{a_0}^2)}{\Gamma[1 + \alpha_{a_0}(t)] \sin[\pi\alpha_{a_0}(t)]}. \quad (11)$$

The scale factor  $s_{scale}$  is fixed at 1 GeV. In addition, the Regge trajectories  $\alpha_{a_0}(t)$  read as  $\alpha_{a_0}(t) = -0.5 \text{ GeV}^2 + 0.6t$  [38, 40].

To describe the behavior of the cross sections at both low and high beam momentum, an interpolating Reggeized treatment will be adopted to interpolate the Regge case smoothly to the Feynman case, which has been successfully applied to several photoproduction processes[27–29, 42–44]. The interpolated Reggeized form factor can then be written as

$$F_t \rightarrow \mathcal{F}_{R,t} = \mathcal{F}_t R(s, t) + F_t [1 - R(s, t)], \quad (12)$$

where  $R(s, t) = R_s(s)R_t(t)$ , with

$$R_s(s) = \frac{1}{1 + e^{-(s-s_R)/s_0}}, \quad R_t(t) = \frac{1}{1 + e^{-(t+t_R)/t_0}}, \quad (13)$$

where  $s_R$  and  $t_R$  are the centroid values for the transition from non-Regge to Regge regimes while  $s_0$  and  $t_0$  describe the respective widths of the transition regions. The four parameters will be fitted to the experimental data. The Feynman-type  $u$  channel will be adopted first in the fitting procedure, and the Rggeized treatment of the  $u$ channel will be discussed in Sec. III C

## III. NUMERICAL RESULTS

With the preparation in the above section, the differential cross section of the  $\pi^- p \rightarrow f_1(1285)n$  reaction will be calculated and compared with the experimental data [22–26]. The

differential cross section in the center-of-mass (c.m.) frame is written as

$$\frac{d\sigma}{d\cos\theta} = \frac{1}{32\pi s} \left| \frac{\vec{k}_2^{\text{c.m.}}}{\vec{k}_1^{\text{c.m.}}} \right| \left( \frac{1}{2} \sum_\lambda |\mathcal{M}|^2 \right), \quad (14)$$

where  $s = (k_1 + p_1)^2$ , and  $\theta$  denotes the angle of the outgoing  $f_1(1285)$  meson relative to the  $\pi$  beam direction in the c.m. frame.  $\vec{k}_1^{\text{c.m.}}$  and  $\vec{k}_2^{\text{c.m.}}$  are the three-momenta of the initial  $\pi$  beam and final  $f_1(1285)$ , respectively. The experimental data for the  $\pi^- p \rightarrow f_1(1285)n$  reaction will be fitted with the help of the MINUIT code in CERNLIB.

### A. $t$ distribution for $\pi^- p \rightarrow f_1(1285)n$ reaction

The interpolating Reggeized treatment is adopted to reproduce the cross section in a beam-momentum region from threshold to several tens of GeV considered in the current work. However, four additional free parameters will be introduced in such treatment. If we recall that at higher beam momenta, the Reggeized  $t$ -channel contribution is dominant, the two parameters  $t_R$  and  $t_0$  can be determined with the  $t$  distribution at a certain beam momentum. Fortunately, there exist experimental data of the  $t$  distribution at beam momentum in the laboratory frame  $P_{Lab} = 12 - 15 \text{ GeV}$  [23]. Hence, we first study  $t$  distribution and determine  $t_R$  and  $t_0$  before making a full fitting of all the data points that we collected.

$t_R$  and  $t_0$  can be determined by the  $t$  distribution because other parameters only affect the  $s$  dependence at high beam momenta. Because the experimental data in Ref. [23] are at a very high beam momentum, one can safely assume that  $R_s(s) \approx 1$ . Hence, one minimizes the  $\chi^2$  per degree of freedom ( $d.o.f.$ ) for the total cross section and the  $t$  distribution of the experimental data at  $P_{Lab} = 12 - 15 \text{ GeV}$  by fitting parameters, which include two parameters for the Regge trajectory  $t_0$  and  $t_R$ . In Ref. [23], the  $t$  distribution is given by the event not the differential cross section, so a scale parameter should be introduced, which can be related to the coupling constant  $g_{a_0 NN}$  with the total cross section which was given in the same Ref. [23] (the total cross section is obtained only by continuation of the  $t$ -channel contribution at very forward angles). The cutoff  $\Lambda_t$  is also involved through Eq. (12). Hence, in the calculation we have four parameters as listed in Table I.

TABLE I. Fitted values of free parameters by fitting the  $t$  distribution in Ref. [23] with a reduced value  $\chi^2/d.o.f. = 0.89$ .

$\Lambda_t$ (GeV)	$g_{a_0 NN}$	$t_0$ (GeV <sup>2</sup> )	$t_R$ (GeV <sup>2</sup> )
$1.26 \pm 0.05$	$28.27 \pm 2.49$	$0.41 \pm 0.16$	$1.90 \pm 1.62$

The fitted values of the free parameters are listed in Table I, with a reduced value of  $\chi^2/d.o.f. = 0.89$ . The best-fitted results are presented in Fig. 2. It is found that the experimental data of the  $t$  distribution for the  $\pi^- p \rightarrow f_1(1285)n$  reaction are well reproduced in our model. Here, we also present the best-fitted results with a pure Feynman model. It confirms that at

high beam momentum, the results with a Feynman model deviate from the experimental data obviously, and the Reggeized treatment is essential to reproduce the  $t$ -slope.

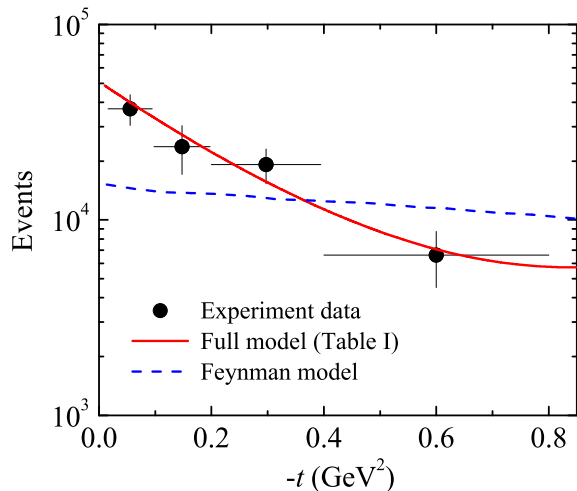


FIG. 2. The  $t$ -distribution for the reaction  $\pi^- p \rightarrow f_1(1285)n$ . The data are from Ref. [23]. The full (red) and dashed (blue) lines are for the full model and Feynman model, respectively.

To show the effect of the interpolating switching function  $R_t(t)$  more clearly, in Fig. 3 we present the results with the values of parameters in Table I. One can see that  $R_t(t)$  is close to 1 at a small value of  $-t$ , which indicates that the contribution of pure Reggeized treatment plays a dominant role at high beam momentum in the  $\pi^- p \rightarrow f_1(1285)n$  reaction.

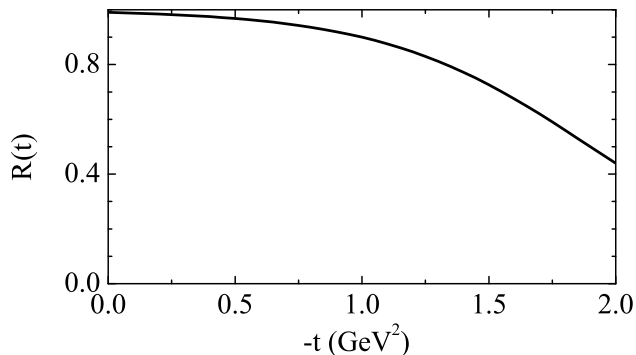


FIG. 3. Interpolating switching function  $R_t(t)$  with the values of parameters in Table I.

Now we would like to give some discussions about the above results. At low beam momentum, the  $R_s(s)$  is very small, which leads to a very small  $R(s, t)$ . Hence, the effect of  $R_t(t)$  should be small at low beam momentum and becomes more important at high momentum where  $R(s, t) \rightarrow R_t(t)$ . At high beam momentum, the  $t$ -channel contribution is usually dominant at very forward angles. At medium and backward angles the  $u$ -channel contribution becomes more important.

The  $t_R$  of  $1.9 \text{ GeV}^2$  in the  $\pi^- p \rightarrow f_1(1285)n$  reaction suggests that at very forward angles the  $R(t)$  is close to 1. Considering that only a few available data points exist, we will assume  $R(t) = 1$  in the following calculation to reduce the number of free parameters. It is reasonable because only the results at a medium angle will be slightly affected where the differential cross section is usually very small.

## B. Cross section of $\pi^- p \rightarrow f_1(1285)n$ reaction

In this subsection, we will fit all the data we collected as shown in Figs. 2 and 4, which include four data points of the total cross section at low beam momentum, three data points of the total cross at high beam momentum, and four data points of the  $t$ -distribution at 12-15 GeV [22–26]. It should be mentioned that the three data points of the total cross section at high beam momentum are obtained by continuation of the  $t$ -channel contribution at very forward angles to all angles, so we will fit these three data points only with the  $t$ -channel contribution because the  $u$ -channel contribution is negligible at forward angles and dominant at backward angles. For the three data points at low beam momentum, both  $t$  and  $u$  channels will be included. It will be found later that the  $s$ -channel contribution is negligible, as usual. We minimize  $\chi^2$  per degree of freedom by fitting five parameters  $s_0$ ,  $s_R$ ,  $\Lambda_t$ ,  $\Lambda_u$  and  $g_{a_0 NN}$  using a total of 11 data points at the beam momentum  $P_{Lab}$  from 2 to 40 GeV as displayed in Fig. 4. Here,  $R(t)$  has been assumed to be 1 as discussed above.

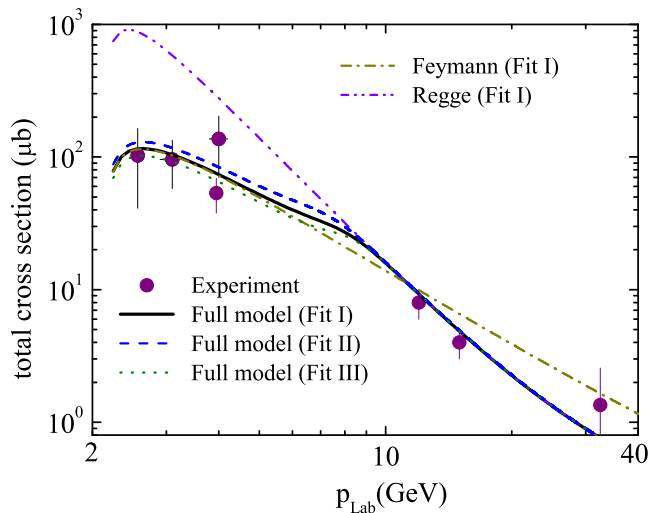


FIG. 4. Total cross section for the  $\pi^- p \rightarrow f_1(1285)n$  reaction. The full (black), dashed (blue), dotted (green) dashed-dotted (dark yellow), and dashed-dot-dotted (violet) lines are for the full model (Fit I), full model (Fit II), full model (Fit III), Feynman case [ $R(s, t) = 0$ ] and Regge case [ $R(s, t) = 1$ ], respectively. The experimental data are from Refs. [22, 24–26].

As observed in Fig. 4, at  $p_{Lab} = 3.95$  and  $4 \text{ GeV}$ , there exist two data points, which are quite different from each other. Because the beam momenta of these two data points are very



TABLE II. Fitted values of free parameters with all 11 data points in Refs. [22–26].

	$\Lambda_t$ (GeV)	$\Lambda_s = \Lambda_u$ (GeV)	$s_0$ (GeV <sup>2</sup> )	$s_R$ (GeV <sup>2</sup> )	$g_{a_0NN}$	$\chi^2/d.o.f.$
Fit I	$1.26 \pm 0.02$	$0.50 \pm 0.78$	$1.53 \pm 0.55$	$14.99 \pm 1.47$	$28.44 \pm 0.08$	1.21
Fit II	$1.27 \pm 0.01$	$0.50 \pm 0.77$	$1.47 \pm 0.38$	$13.76 \pm 1.38$	$28.44 \pm 0.11$	1.18
Fit III	$1.25 \pm 0.01$	$0.50 \pm 0.77$	$1.35 \pm 0.32$	$15.46 \pm 1.36$	$28.44 \pm 0.07$	1.16

close, it is difficult to interpret them as a physical structure. We present the results by fitting with both data points at a beam momentum of about 4 GeV (Fit I), the results with a higher momentum (Fit II) and the results with a lower momentum (Fit III). The results suggest that the higher data point is difficult to reproduce in three fits, whose results are close to each other and support the lower data point. The fitted parameters are listed in Table II, and the values of the coupling constant  $g_{a_0NN}$  and cutoff  $\Lambda_t$  are close to those in Table I. We also present the results of the usual Feynman case [ $R(s, t) = 0$ ] and Regge case [ $R(s, t) = 1$ ] in Fig. 4, which show that the experimental data of the total cross section of the  $\pi^- p \rightarrow f_1(1285)n$  reaction cannot be reproduced using the Feynman model alone, even with the traditional Reggeized treatment. The interpolating Reggeized treatment is essential to reproduce the total cross section at both low and high beam momenta.

In Fig. 5, we present the explicit results with Fit I. The results show that the experimental data of both the total and  $t$  distribution can be well reproduced in our model. The  $t$ -channel contribution is dominant at  $p_{lab}$  up to about 20 GeV. The  $u$ -channel contribution is negligible compared with the  $t$ -channel contribution at low beam momenta, but becomes more important and exceeds the  $t$ -channel contribution at a beam momentum of about 30 GeV.

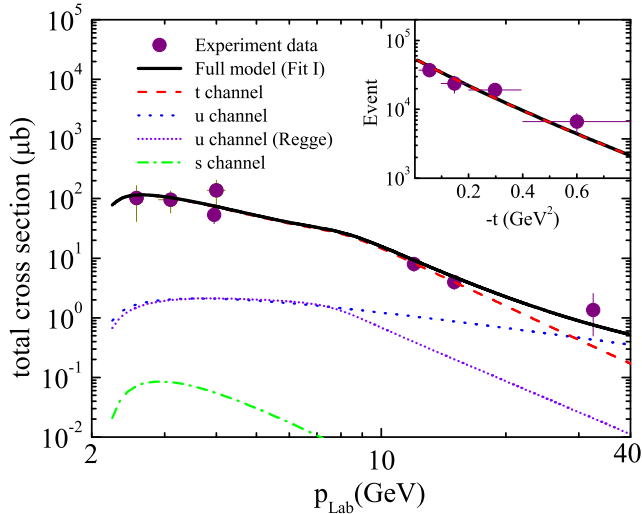


FIG. 5. Total cross section for the  $\pi^- p \rightarrow f_1(1285)n$  reaction. The full (black), dashed (red), dotted (blue), short-dotted (violet), and dashed-dotted (green) lines are for the full model (Fit I),  $t$  channel,  $u$  channel,  $u$  channel with interpolated Reggeized treatment and  $s$  channel, respectively. The experimental data are from Refs. [22–26].

The  $u$ -channel contribution can be seen more clearly in the differential cross section as shown in Fig. 6. The  $t$  and  $u$  chan-

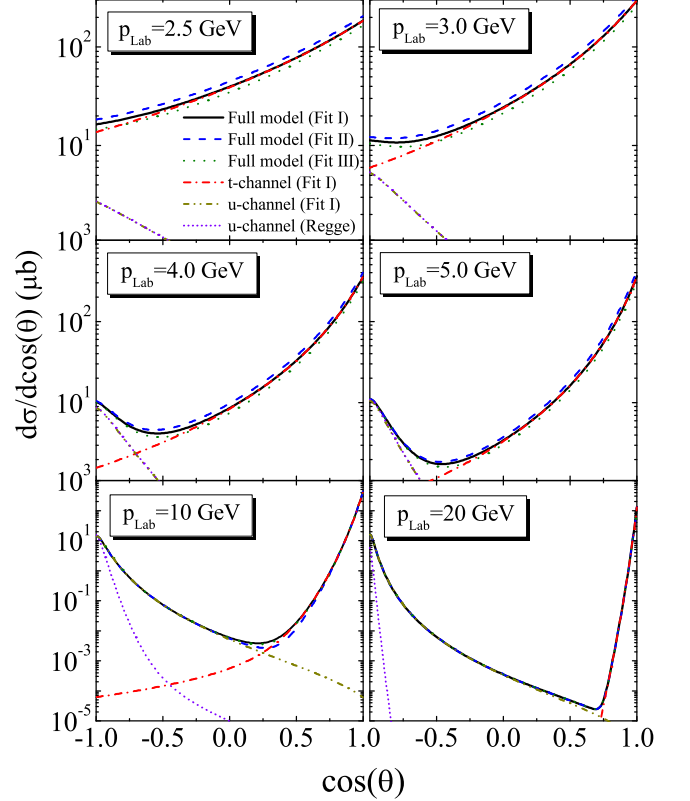


FIG. 6. The differential cross section  $d\sigma/d\cos\theta$  of the  $\pi^- p \rightarrow f_1(1285)n$  interaction as a function of  $\cos\theta$ . The full (black), dashed (blue), dotted (green), dashed-dotted (red), dashed-dot-dotted (dark yellow), and short-dotted (violet) lines are for the full model (Fit I), full model (Fit II), full model (Fit III),  $t$  channel (Fit I),  $u$  channel (Fit I), and  $u$  channel with interpolated Reggeized treatment.

nels appear at forward and backward angles as expected. At low beam momentum, the differential cross section is dominated by the  $t$  channel at a large range of the angles, whose contribution decreases with the decrease of the  $\cos\theta$ . At momenta lower than about 3 GeV, the  $t$  channel is more important than the  $u$  channel even at extreme backward angles. At the beam momenta higher than about 3 GeV, the  $u$  channel becomes more and more important with the increase of the beam momentum. At a beam momentum of 20 GeV, though the total cross section is still mainly from the  $t$ -channel contribution, the  $u$  channel is dominant even at medium angles while the  $t$

channel is only dominant at very forward angles. The results of the three fits are also presented in Fig. 6. The discrepancy of the differential cross sections of three fits is small at most beam momenta.

### C. Reggeized $u$ -channel contribution

In the above calculation, the Reggeized treatment is applied to the  $t$  channel, but not to the  $u$  channel. Physically, the  $u$  channel can be seen as a  $t$  channel with the final particles interchanged. Hence, the Reggeized treatment should be adopted in the  $u$  channel, and as in the  $t$  channel the interpolated treatment is needed to connect the Regge case at high beam momentum smoothly to the Feynman case at low beam momentum [45, 46]. Since the experimental data at high beam momenta are only obtained from the  $t$ -channel contribution, the fitting procedure in the above is not affected by the inclusion of the interpolated Reggeized  $u$ -channel contribution, whose contribution at low beam momentum is just the Feynman type that we adopted in the above fitting procedure. However, the different treatment of the  $u$  channel will affect prediction of the cross section at a high beam momentum, which will be discussed in this subsection.

The Reggeized treatment for  $u$ -channel baryon exchange consists of replacing the form factor  $F_u(u)$  in Eq. (10) as

$$\mathcal{F}_u(u) = \left(\frac{s}{s_{scale}}\right)^{\alpha_N(u)-\frac{1}{2}} \frac{\pi\alpha'_N(u - m_N^2)}{\Gamma[\frac{1}{2} + \alpha_N(u)] \sin[\pi(\alpha_N(u) - \frac{1}{2})]}. \quad (15)$$

The scale factor  $s_{scale}$  is fixed at 1 GeV. In addition, the Regge trajectories  $\alpha_N(u)$  read [47]

$$\alpha_N(u) = -0.34 \text{ GeV}^2 + 0.99u. \quad (16)$$

The interpolating can be applied to the  $u$  channel analogously to the  $t$  channel by replacing  $t$  with  $u$ . It is reasonable to assume that the Reggeized treatment begins to exhibit its effect at the same value of beam momentum for both the  $t$  channel and  $s$  channel. So, we adopt the same parameters in the interpolating treatment for the  $t$  channel as those for the  $s$  channel. As said above, the fitting procedure is not affected with the inclusion of the interpolated Reggeized treatment in the  $u$  channel. In this work, coupling constants involved in the  $u$  channel are fixed at the values in our previous work [21]. The  $u$  channel at high beam momentum is determined after the cutoff  $\Lambda_u$  is fixed in the fitting of the experimental data. In Fig. 5, the numerical results of the total cross section of the  $u$  channel with interpolated Reggeized treatment are presented. As expected, it decreases exponentially as the  $t$  channel at high beam momentum and is much smaller than those without Reggeized treatment. However, the small contribution of the Reggeized  $u$  channel does not mean that its contribution is

negligible in the differential cross section. As shown in Fig. 6, the  $u$  channel plays an important role in shaping the differential cross section at backward angles at high beam momentum. The results in the full model are almost the sum of the  $u$ - and  $t$ -channel contributions, which are not given explicitly in the figures. Most of the  $f(1285)$  events are at extreme forward and backward angles, which correspond to the Reggeized  $t$  and  $u$  channel, respectively. At low beam momentum, the results with interpolated Reggeized treatment are almost the same as those with the Feynman type.

## IV. SUMMARY AND DISCUSSION

In this work, based on the existing experimental data, we analyze the  $\pi^- p \rightarrow f_1(1285)n$  reaction with an interpolating Reggeized approach and try to make a prediction of its total and differential cross sections at a large beam-momentum range from threshold up to several tens of GeV. It is found that a pure Feynman or pure Regge type of  $t$ -channel contribution cannot reproduce the existing experiment data, though there are only 11 data points against 5 free parameters. The interpolating Reggeized treatment is essential to reproduce the cross sections at both low and high beam momenta.

At low momenta, both total and differential cross sections are dominant with the Feynman-type  $t$  channel. At high beam momenta, the Reggeized  $t$ -channel contribution is only dominant at extreme forward angles and decays rapidly with the decrease of  $\cos\theta$ . The  $u$ -channel contributions with and without Reggeized treatment exhibit quite different behaviors at a high beam momentum. Without the Reggeized treatment, the  $u$  channel becomes important in a larger range of angles with the increase of the beam momentum, while the  $t$  channel plays its role only at a very forward angle at high beam momenta. With the Reggeized treatment, the  $u$  channel and  $t$  channel provide a sharp increase and a sharp decrease at extreme backward and extreme forward angles, respectively.

The low- and high-momentum pion beams are accessible at the J-PARC and COMPASS. Our result is helpful to the possible experimental research of  $f_1(1285)$  at the two facilities. Based on the results, the measurement at forward angles is supported while a measurement at extreme backward angles is helpful to understand the interaction mechanism of the pion-induced  $f_1(1285)$  production.

## V. ACKNOWLEDGMENTS

This project is supported by the National Natural Science Foundation of China under Grant No. 11675228 and the Major State Basic Research Development Program in China under Grant No. 2014CB845405.

[1] F. K. Guo, C. Hanhart, U. G. Meier, Q. Wang, Q. Zhao and B. S. Zou, "Hadronic molecules," arXiv:1705.00141 [hep-ph].

[2] J. Dudek *et al.*, "Physics Opportunities with the 12 GeV Upgrade at Jefferson Lab," *Eur. Phys. J. A* **48**, 187 (2012)

- [3] S. Kumano, "Spin Physics at J-PARC," *Int. J. Mod. Phys. Conf. Ser.* **40**, 1660009 (2016)
- [4] F. Nerling [COMPASS Collaboration], "Hadron Spectroscopy with COMPASS: Newest Results," *EPJ Web Conf.* **37**, 01016 (2012)
- [5] C. Patrignani *et al.* [Particle Data Group], "Review of Particle Physics," *Chin. Phys. C* **40**, no. 10, 100001 (2016).
- [6] L. Roca, E. Oset and J. Singh, "Low lying axial-vector mesons as dynamically generated resonances," *Phys. Rev. D* **72**, 014002 (2005)
- [7] L. S. Geng, X. L. Ren, Y. Zhou, H. X. Chen and E. Oset, "*S*-wave  $KK^*$  interactions in a finite volume and the  $f_1(1285)$ ," *Phys. Rev. D* **92**, no. 1, 014029 (2015)
- [8] Y. Zhou, X. L. Ren, H. X. Chen and L. S. Geng, "Pseudoscalar meson and vector meson interactions and dynamically generated axial-vector mesons," *Phys. Rev. D* **90**, no. 1, 014020 (2014)
- [9] S. K. Choi *et al.* [Belle Collaboration], "Observation of a narrow charmonium-like state in exclusive  $B^+ \rightarrow K^+\pi^+\pi^-J/\psi$  decays," *Phys. Rev. Lett.* **91**, 262001 (2003)
- [10] M. Ablikim *et al.* [BESIII Collaboration], "Observation of a Charged Charmoniumlike Structure in  $e^+e^- \rightarrow \pi^+\pi^-J/\psi$  at  $\sqrt{s} = 4.26\text{GeV}$ ," *Phys. Rev. Lett.* **110**, 252001 (2013)
- [11] M. Ablikim *et al.* [BESIII Collaboration], "Observation of a charged charmoniumlike structure in  $e^+e^- \rightarrow (D^*\bar{D}^*)^\pm\pi^\mp$  at  $\sqrt{s} = 4.26\text{GeV}$ ," *Phys. Rev. Lett.* **112**, no. 13, 132001 (2014)
- [12] A. Bondar *et al.* [Belle Collaboration], "Observation of two charged bottomonium-like resonances in  $Y(5S)$  decays," *Phys. Rev. Lett.* **108**, 122001 (2012)
- [13] P. L. Lü and J. He, "Hadronic molecular states from the  $K\bar{K}^*$  interaction," *Eur. Phys. J. A* **52**, no. 12, 359 (2016)
- [14] J. He, "Study of the  $B\bar{B}^*/D\bar{D}^*$  bound states in a Bethe-Salpeter approach," *Phys. Rev. D* **90**, 076008 (2014)
- [15] J. He, "The  $Z_c(3900)$  as a resonance from the  $D\bar{D}^*$  interaction," *Phys. Rev. D* **92**, 034004 (2015)
- [16] J. He, X. Liu, Z. F. Sun and S. L. Zhu, " $Z_c(4025)$  as the hadronic molecule with hidden charm," *Eur. Phys. J. C* **73**, 2635 (2013)
- [17] Z. F. Sun, J. He, X. Liu, Z. G. Luo and S. L. Zhu, " $Z_b(10610)^\pm$  and  $Z_b(10650)^\pm$  as the  $B^*\bar{B}$  and  $B^*\bar{B}^*$  molecular states," *Phys. Rev. D* **84**, 054002 (2011)
- [18] Z. F. Sun, Z. G. Luo, J. He, X. Liu and S. L. Zhu, "A note on the  $B^*$  anti- $B$ ,  $B^*$  anti- $B^*$ ,  $D^*$  anti- $D$ ,  $D^*$  anti- $D^*$ , molecular states," *Chin. Phys. C* **36**, 194 (2012).
- [19] R. Dickson *et al.* [CLAS Collaboration], "Photoproduction of the  $f_1(1285)$  Meson," *Phys. Rev. C* **93**, no. 6, 065202 (2016)
- [20] Y. Y. Wang, L. J. Liu, E. Wang and D. M. Li, "Study on the reaction of  $\gamma p \rightarrow f_1(1285)p$  in Regge-effective Lagrangian approach," *Phys. Rev. D* **95**, 096015 (2017)
- [21] X. Y. Wang and J. He, "Analysis of recent CLAS data on  $f_1(1285)$  photoproduction," *Phys. Rev. D* **95**, 094005 (2017)
- [22] O. I. Dahl, L. M. Hardy, R. I. Hess, J. Kirz and D. H. Miller, "Strange-particle production in  $\pi$ - $p$  interactions from 1.5 to 4.2 BeV/c. I. Three-and-more-body final states," *Phys. Rev.* **163**, 1377 (1967).
- [23] M. J. Corden *et al.*, "Observation of the  $D$ ,  $e$  and Delta Mesons in  $\pi^-p$  Interactions at 12-GeV/c and 15-GeV/c," *Nucl. Phys. B* **144**, 253 (1978).
- [24] C. Dionisi *et al.* [CERN-College de France-Madrid-Stockholm Collaboration], "Observation and Quantum Numbers Determination of the E(1420) Meson in  $\pi$ - $p$  Interactions at 3.95-GeV/c," *Nucl. Phys. B* **169**, 1 (1980).
- [25] S. I. Bitukov *et al.*, "Investigation of  $D(1285)$  and  $e(1420)$  Mesons Production in Exclusive Interactions of  $\pi^-$  and  $K^-$  Mesons at 32.5-GeV/c," *Sov. J. Nucl. Phys.* **39**, 735 (1984) [*Yad. Fiz.* **39**, 1165 (1984)].
- [26] S. I. Bitukov *et al.*, "Observation of  $D(1285) \rightarrow \phi\gamma$  Radiative Decay," *Phys. Lett. B* **203**, 327 (1988).
- [27] S. I. Nam and C. W. Kao, " $\Lambda(1520)$  photoproduction off the proton target with Regge contributions," *Phys. Rev. C* **81**, 055206 (2010)
- [28] J. He, " $\Sigma(1385)$  photoproduction from proton within a Regge-plus-resonance approach," *Phys. Rev. C* **89**, no. 5, 055204 (2014)
- [29] J. He, "Theoretical study of the  $\Lambda(1520)$  photoproduction off proton target based on the new CLAS data," *Nucl. Phys. A* **927**, 24 (2014)
- [30] X. H. Liu, Q. Zhao and F. E. Close, "Search for tetraquark candidate  $Z(4430)$  in meson photoproduction," *Phys. Rev. D* **77**, 094005 (2008)
- [31] G. Penner and U. Mosel, "Vector meson production and nucleon resonance analysis in a coupled channel approach for energies  $m(N)$  less than  $s^{*(1/2)}$  less than 2-GeV. I. Pion induced results and hadronic parameters," *Phys. Rev. C* **66**, 055211 (2002)
- [32] P. Colangelo and F. De Fazio, "Open charm meson spectroscopy: Where to place the latest piece of the puzzle," *Phys. Rev. D* **81**, 094001 (2010)
- [33] K. Tsushima, A. Sibirtsev, A. W. Thomas and G. Q. Li, "Resonance model study of kaon production in baryon baryon reactions for heavy ion collisions," *Phys. Rev. C* **59**, 369 (1999) Erratum: [*Phys. Rev. C* **61**, 029903 (2000)]
- [34] Z. W. Lin, C. M. Ko and B. Zhang, "Hadronic scattering of charm mesons," *Phys. Rev. C* **61**, 024904 (2000)
- [35] V. Baru, C. Hanhart, M. Hoferichter, B. Kubis, A. Nogga and D. R. Phillips, "Precision calculation of threshold  $\pi$ - $d$  scattering,  $\pi$  N scattering lengths, and the GMO sum rule," *Nucl. Phys. A* **872**, 69 (2011)
- [36] S. K. Domokos, H. R. Grigoryan and J. A. Harvey, "Photoproduction through Chern-Simons Term Induced Interactions in Holographic QCD," *Phys. Rev. D* **80**, 115018 (2009)
- [37] M. Birkel and H. Fritzsche, "The Nucleon spin and the mixing of axial vector mesons," *Phys. Rev. D* **53**, 6195 (1996)
- [38] N. I. Kochelev, M. Battaglieri and R. De Vita, "Exclusive photoproduction of  $f_1(1285)$  meson off proton in the JLab kinematics," *Phys. Rev. C* **80**, 025201 (2009)
- [39] J. He and B. Saghai, " $\eta$  production off the proton in a Regge-plus-chiral quark approach," *Phys. Rev. C* **82**, 035206 (2010)
- [40] G. Galata, "Photoproduction of  $Z(4430)$  through mesonic Regge trajectories exchange," *Phys. Rev. C* **83**, 065203 (2011)
- [41] X. Y. Wang and J. He, " $K^{*0}\Lambda$  photoproduction off a neutron," *Phys. Rev. C* **93**, 035202 (2016)
- [42] H. Haberzettl, X. Y. Wang and J. He, "Preserving Local Gauge Invariance with t-Channel Regge Exchange," *Phys. Rev. C* **92**, 055503 (2015)
- [43] X. Y. Wang, J. He and H. Haberzettl, "Analysis of recent CLAS data on  $\Sigma^*(1385)$  photoproduction off a neutron target," *Phys. Rev. C* **93**, 045204 (2016)
- [44] J. He and X. R. Chen, "The roles of nucleon resonances in  $\Lambda(1520)$  photoproduction off proton," *Phys. Rev. C* **86**, 035204 (2012)
- [45] S. H. Kim, A. Hosaka, H. C. Kim, and H. Noumi, "Production of strange and charmed baryons in pion induced reactions," *Phys. Rev. D* **92**, 094021 (2015).
- [46] B. G. Yu, T. K. Choi, and W. Kim, "Regge phenomenology of pion photoproduction off the nucleon at forward angles," *Phys. Rev. C* **83**, 025208 (2011).
- [47] J. K. Storrow, "Baryon exchange processes," *Phys. Rep.* **103**, 317 (1984).